Paper AAS 03-569

Application of Local Lyapunov Exponents to Maneuver Design and Navigation in the Three-Body Problem

Rodney L. Anderson
The Colorado Center for Astrodynamics Research
University of Colorado
Boulder, CO 80309

Martin W. Lo
Jet Propulsion Laboratory
California Institute of Technology
Pasadena, CA 91109

George H. Born
The Colorado Center for Astrodynamics Research
University of Colorado
Boulder, CO 80309

AAS/AIAA Astrodynamics Specialist Conference

Big Sky Resort, Big Sky, Montana, August 3-7, 2003

AAS Publications Office, P.O. Box 28130, San Diego, CA 92198

AAS 03-569

APPLICATION OF LOCAL LYAPUNOV EXPONENTS TO MANEUVER DESIGN AND NAVIGATION IN THE THREE-BODY PROBLEM

Rodney L. Anderson,* Martin W. Lo,† George H. Born*

Dynamical systems theory has recently been employed to design trajectories within the three-body problem for several missions. This research has applied one stability technique, the calculation of local Lyapunov exponents, to such trajectories. Local Lyapunov exponents give an indication of the effects that perturbations or maneuvers will have on trajectories over a specified time. A numerical comparison of local Lyapunov exponents was first made with the distance random perturbations traveled from a nominal trajectory, and the local Lyapunov exponents were found to correspond well with the perturbations that caused the greatest deviation from the nominal. This would allow them to be used as an indicator of the points where it would be important to reduce navigation uncertainties. The ΔV required to return to a nominal trajectory from a random perturbation was also used in the comparison, and it was found that a relationship existed between the local Lyapunov exponents and the maximum ΔV required to return to the nominal trajectory from the random perturbation. This information has possible applications to maneuver design on unstable orbits.

INTRODUCTION

New methods have recently been developed using dynamical systems theory in an effort to aid in the design of trajectories within the three-body problem. These techniques have been applied to trajectory design for several different missions. These missions include the Genesis mission, which has successfully traveled along the initial portion of its trajectory.[1, 2] Several earlier missions utilized libration-point orbits beginning with ISEE-3 in 1978.[3] As quasi-periodic orbits are used for an increasing number of missions, it is desirable to develop techniques that can aid in navigation and enable maneuver design on these types of orbits.

*The Colorado Center for Astrodynamics Research, University of Colorado, Boulder, CO 80309
†Jet Propulsion Laboratory, California Institute of Technology, Pasadena, CA 91109

Stationkeeping for quasi-periodic orbits in the three-body problem has previously been studied using several different techniques. Stationkeeping for ISEE-3 consisted of several large maneuvers on the order of 10 m/s spaced at greater than two-week intervals.[3, 4] Howell and Pernicka developed an algorithm to keep a spacecraft close to a nominal Lissajous orbit and to estimate the ΔV required to remain close to that desired orbit.[5] Their algorithm resulted in ΔVs on the order of 0.1 m/s with time intervals of one to two months; note that their study was performed in the Sun-Earth/Moon system, while the current paper uses the Earth-Moon system. In their research, the selection of epochs for these maneuvers was mentioned as an area for further study. Scheeres and Renault examined stationkeeping maneuvers and looked at the optimal time interval between maneuvers.[6] Using a different approach, Simó et al. applied Floquet theory to quasi-periodic libration orbits in order to search for a more dynamical approach to maneuver design.[7] The use of Floquet theory limits the application of this technique to periodic and quasi-periodic orbits in the three-body problem. Gómez, Howell, Masdemont, and Simó performed a comparison of the Floquet approach with the method developed by Howell and Pernicka in the Earth-Moon system.[8] The ΔVs in Gómez et al.'s approach were on the order of several cm/s with time intervals of one to several days. In another area of research, the sensitivity of trajectories has been analyzed for the Genesis trajectory by Bell, Lo, and Wilson.[9]

A possible method for examining the effectiveness of maneuvers on a trajectory and the influence of perturbations would be to apply stability techniques, such as the use of local Lyapunov exponents, to the three-body problem. Local Lyapunov exponents are based on the concepts introduced by Lyapunov[10] in 1892. Later, Oseledec[11] introduced a theorem that was used by Abarbanel et al.[12] to define and calculate local Lyapunov exponents in several different types of systems. See Froeschlé et al. for applications to dynamical astronomy and references.[13] In the current study these methods have been implemented and applied to trajectories in the three-body problem. In this paper, a description of how local Lyapunov exponents vary is given first. The calculated local Lyapunov exponents are then compared to the effects of random perturbations to a trajectory. Finally, possible applications to maneuver design are investigated by determining how the local Lyapunov exponents relate to the ΔVs required to return to a nominal trajectory from randomly perturbed states. Such techniques may contribute to the automation of the navigation and maneuver design process on unstable orbits in the future.

METHOD

Local Lyapunov Exponents

Local Lyapunov exponents are used to determine the behavior of nearby trajectories over a finite time. This is equivalent to quantifying the effect of a perturbation to a nominal trajectory at a selected location; this would give an indication of where it would be most important to reduce uncertainties in a spacecraft's state. The information obtained from local Lyapunov exponents can also be used to show how the ΔV required to return to a nominal trajectory for a given perturbation varies along the trajectory. The primary area of interest in this study was in the maximum effect of perturbations and the worst case maneuver ΔV required to return to the nominal trajectory, so the calculations were limited to finding the maximum local Lyapunov exponent. This method produces an easily computed value that can be used as a metric to give a qualitative indication of how stability varies over a trajectory. These results reveal areas of interest along a trajectory where additional quantities necessary for taking advantage of this information could be calculated. Such quantities would relate to the direction of the perturbations, but these quantities have not yet been included in this analysis. These techniques are applicable to quasi-periodic orbits, which is the focus of the current study, as well as other trajectories in the three-body problem. They can also be extended to include trajectories in the n-body problem and continuous thrust trajectories. A discussion of Lyapunov exponents will be given next as an introduction to local Lyapunov exponents. The equation for computing local Lyapunov exponents can then be obtained in a straightforward manner from the Lyapunov exponent equation.

Lyapunov exponents are used to measure the convergence or divergence of nearby trajectories in a dynamical system.[14] They characterize the dynamical system as a whole and do not depend on any specific orbit. Lyapunov exponents also reveal how infinitesimal perturbations will behave over long time periods rather than short ones. Generally, Lyapunov exponents measure how random a system is or its stochasticity. A positive value for the Lyapunov exponent usually indicates that nearby trajectories will diverge and that the flow is chaotic. Here, the flow of the differential equations is used to refer to the global set of trajectories in a system. The discussion of Lyapunov exponents below follows Oseledec[11] and Abarbanel et al.[12]

Lyapunov exponents deal with the difference $\delta \boldsymbol{x}$ between two nearby solutions of the flow. They give insight into the growth in this distance over time for flows. Let

$$\dot{\boldsymbol{x}}(t) = f(\boldsymbol{x}, t) \tag{1}$$

represent the equations of motion. Then the linearized equations of motion (variational equations) are given by[15]

$$\delta \boldsymbol{x}(t) = \Phi(t, t_o)\delta \boldsymbol{x}(t_o) \tag{2}$$

where $\Phi(t, t_o)$ is the state transition matrix. Lyapunov exponents are similar to characteristic numbers which can be defined for a scalar valued function φ_t as

$$\lim_{t \to \pm\infty} \frac{1}{|t|} \ln |\varphi_t|. \tag{3}$$

Here, there are characteristic numbers for both $t \to +\infty$ and $t \to -\infty$, while $|\cdot|$ denotes the Euclidean norm. In his definition of the Lyapunov exponent, Oseledec defines a norm in Euclidean space $\mathbb{R}^d$ for some matrix $\boldsymbol{a}$ (a linear operator) as

$$||\boldsymbol{a}|| = \text{maximum eigenvalue of } \sqrt{\boldsymbol{a} \cdot \boldsymbol{a}^T}. \tag{4}$$

This is equivalent to the operator norm

$$\|\boldsymbol{a}\| = \sqrt{\text{max. eigenvalue of } \boldsymbol{a} \cdot \boldsymbol{a}^T} = \sup_{|\boldsymbol{u}|=1} |\boldsymbol{a}(\boldsymbol{u})| \tag{5}$$

where sup is the supremum or least upper bound and $\mathbf{a}\cdot\mathbf{a}^{\mathbf{T}}$ forms a symmetric matrix.[16] The operator norm gives the maximum amount by which the operator $\boldsymbol{a}$ stretches $\boldsymbol{u}$. Oseledec then proceeds to show that the Lyapunov exponents do not depend on the norm that is used, or that they are affine invariants. Using this definition, the Lyapunov exponent for a flow may be defined as

$$\Lambda = \lim_{\substack{t-t_0\to\infty \\ |\delta\boldsymbol{x}(t_0)|\,\to\,0}} \frac{1}{t-t_0} \ln \frac{|\delta\boldsymbol{x}(t)|}{|\delta\boldsymbol{x}(t_0)|}. \tag{6}$$

The state transition matrix acts like the linear operator $\boldsymbol{a}$ on some infinitesimal initial perturbation $\delta\boldsymbol{x}(t_0)$ to give the growth of the perturbation at a later time. Thus, the equation for calculating Lyapunov exponents may be written in terms of $\Phi(t, t_0)$.

$$\Lambda = \lim_{t-t_0\to\infty} \frac{1}{t-t_0} \ln \|\Phi(t, t_0)\| \tag{7}$$

Now, when the flow is integrated over n time steps Eq. (7) becomes

$$\Lambda = \lim_{n\Delta t\to\infty} \frac{1}{n\Delta t} \ln \|\Phi(n\Delta t + t_0, t_0)\|. \tag{8}$$

If instead of taking the limit, the computation is stopped after n time steps, the equation for calculating the local Lyapunov exponents (λ) is obtained:

$$\lambda = \frac{1}{n\Delta t} \ln \|\Phi(n\Delta t + t_0, t_0)\| \tag{9}$$

or

$$\lambda = \frac{1}{n\Delta t} \ln \left(\text{max. eigenvalue of } \sqrt{\Phi(n\Delta t + t_0, t_0)\Phi^T(n\Delta t + t_0, t_0)}\right). \tag{10}$$

Local Lyapunov exponents are used to examine the flow over a finite time, so removing the limit in the Lyapunov exponent calculation to obtain them makes sense. They are calculated by integrating the state transition matrix on a specific trajectory over a chosen number of time steps. This allows the desired variation in stability over the system to be examined rather than just producing the one result describing the whole system that is given by the usual Lyapunov exponents. The resulting local Lyapunov exponents possess the same characteristics of Lyapunov exponents in that larger values indicate that nearby trajectories will diverge more quickly. The use of the operator norm gives the maximum growth of the perturbation, which is the desired output for this study. Abarbanel et al. argue for the use of this norm,[12] and it possesses the additional benefit that it eliminates the requirement for calculating the eigenvectors. It will also be numerically well-behaved. A similar concept to local Lyapunov exponents called "finite time Lyapunov characteristic exponents" does not use the operator norm. Scheeres et al. make use of these finite time Lyapunov characteristic exponents to indicate how the frequency of measurements might affect the uncertainties along an unstable orbit.[17]

Dynamic Models

The calculation of local Lyapunov exponents were initially applied in the circular restricted three-body problem (CR3BP). In this model, two bodies (the primaries, P_1 and P_2) are assumed to travel about their center of mass in circular orbits. The problem is to determine the motion of a third infinitesimal mass (P_3) that has a negligible effect on the motion of the two primaries. A diagram of the problem is shown in Figure 1 with the primary possessing the larger mass (P_1) shown on the left. An inertial coordinate system

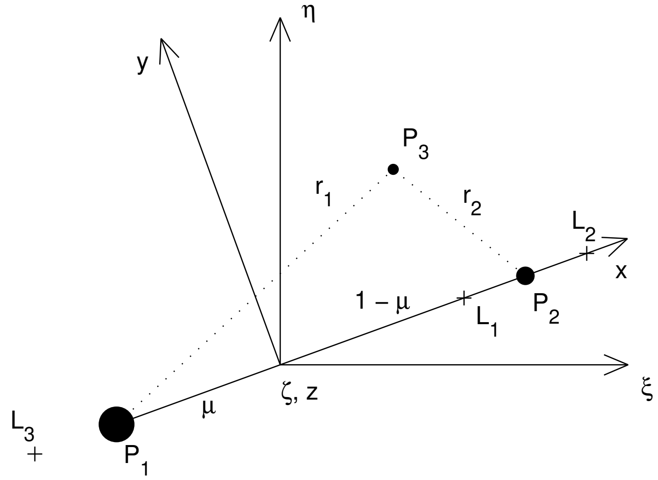

Figure 1 Diagram of the Circular Restricted Three-Body Problem

(ξ,η,ζ) and a rotating coordinate system (x, y, z) are placed with their centers at the center of mass of the two primaries. The rotating coordinate system rotates with the mean motion of the primaries so that its x-axis always points from P_1 to P_2. The various quantities used in the CR3BP are typically nondimensionalized so that the mass of the smaller primary is defined to be μ with the mass of the larger primary given by $1-\mu$. The distance from the origin to P_1 is then μ, and the distance from the origin to P_2 is $1-\mu$. The nondimensional time corresponds to the angular distance traveled by the primaries. The equations of motion for the infinitesimal mass in the rotating coordinate system may then be written as

$$\ddot{x} - 2\dot{y} = x - (1-\mu)\frac{x - x_1}{{r_1}^3} - \mu\frac{x - x_2}{{r_2}^3} \tag{11}$$

$$\ddot{y} + 2\dot{x} = \left(1 - \frac{(1-\mu)}{{r_1}^3} - \frac{\mu}{{r_2}^3}\right) y \tag{12}$$

$$\ddot{z} = -\left(\frac{(1-\mu)}{{r_1}^3} - \frac{\mu}{{r_2}^3}\right) z. \tag{13}$$

Here, r_1 is the distance between the infinitesimal mass and P_1, and r_2 is the distance between the infinitesimal mass and P_2. The x-axis locations of P_1 and P_2 are x_1 and x_2.

The equilibrium points in this problem are typically referred to as Lagrange points, and it is at these points that periodic orbits have been found to exist. The collinear Lagrange points (L1, L2, and L3) are labeled in Figure 1. In this paper, the Lagrange points in the Earth-Moon system are referred to as Lunar Lagrange points, so L1 is called Lunar L1 or LL1. In the three-body problem, these orbits become quasi-periodic or Lissajous orbits. The trajectories used in this study consist of these types of orbits.

The calculation of local Lyapunov exponents was also implemented in JPL's libration point mission design tool (LTool) in order to examine trajectories in the three-body problem. This tool has the ability to include the DE-405 ephemerides[18] for the selected bodies as well as algorithms to aid in computing quasi-periodic orbits. The initial conditions for the Lissajous orbit were obtained using the Richardson-Cary expansion algorithm.[19] The initial conditions for the Lyapunov orbits were computed using AUTO2000 scripts provided by Paffenroth.[20] LTool's differential corrector then used these initial conditions to obtain a continuous orbit while incorporating the ephemerides.

RESULTS

Calculation of Local Lyapunov Exponents on Selected Trajectories

In order to obtain a better understanding of the behavior of local Lyapunov exponents, they were computed along various periodic and quasi-periodic orbits using the two different dynamic models. The local Lyapunov exponents were typically calculated at 0.1-day time steps for these orbits in the Earth-Moon system. At each of these points a selected time interval, such as one day, was used in the local Lyapunov exponent calculation. The different time intervals are illustrated in Figure 2. In this figure, the dots are placed on the trajectory at the time interval used between the calculation of the local Lyapunov exponents. The larger interval represents the time period used in the local Lyapunov exponent calculation.

As a first step, trajectories in the CR3BP were examined. The results from LTool for a Lyapunov orbit around the LL1 libration point using this model are shown in Figure 3. In this plot, the trajectory is shown in the rotating coordinate frame, and the magnitude of the local Lyapunov exponents, which were calculated over one-day time periods, is represented by the color gradient. The local Lyapunov exponents are also plotted as arrows perpendicular to the trajectory with the scale indicated on the plot. So the magnitude of the local Lyapunov exponents in this plot indicates the effect a perturbation to a trajectory would be expected to have over one day. The direction of the arrows have no physical meaning and are for ease of visualization only. A plot of the local Lyapunov exponents versus time is also given in Figure 4. It can be seen that the largest peak in the local Lyapunov exponents with a magnitude of nearly three days^{-1} (λ is in units of 1/days) occurs nearest the Moon. The local Lyapunov exponents rise as the trajectory approaches the Moon. If smaller time intervals are used for the local Lyapunov exponent calculation, the peak will be centered closer to the Moon. A similar trend occurs on the side of the orbit closest to the Earth. This makes sense because these locations correspond to the points on the orbits that would be most perturbed by the gravitating bodies.

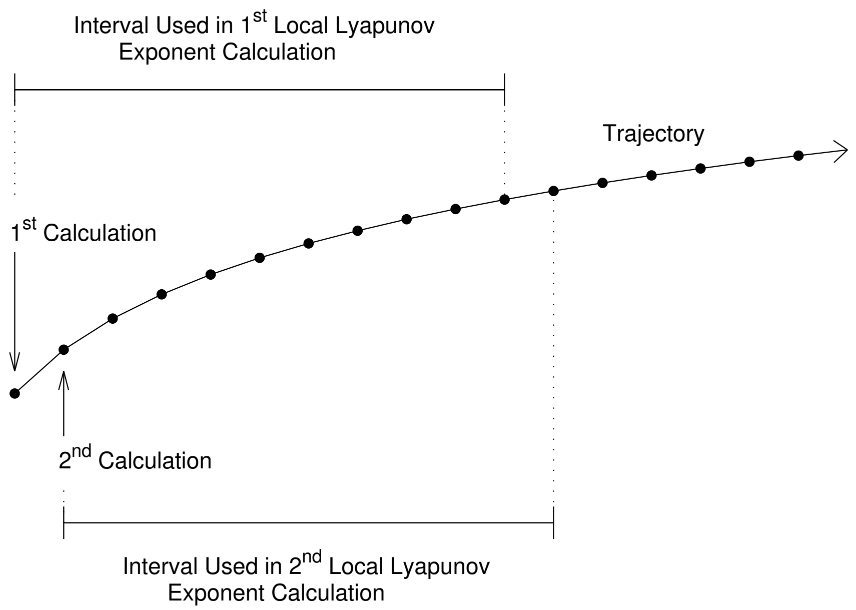

Figure 2 Illustration of the Time Intervals Used in the Local Lyapunov Exp. Calculation

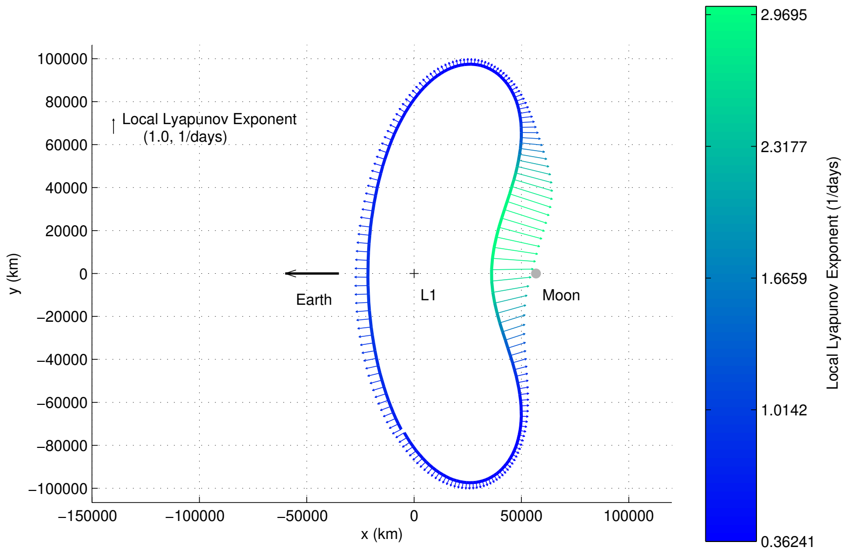

Figure 3 Local Lyapunov Exponents Calculated Over One-Day Intervals on a Planar Lyapunov Orbit in the Earth-Moon System using the CR3BP Model (Arrows indicate the magnitude of the local Lyapunov exponents with the scale given in the upper left corner.)

Next, the local Lyapunov exponents were calculated over one-day intervals for a Lissajous orbit in the Earth-Moon system including the ephemerides as shown in Figure 5. A plot versus time over approximately one period is also given in Figure 6 for this Lissajous orbit. The highest peak corresponds to the increased local Lyapunov exponents closest to the Moon, and the second highest peak corresponds to the local Lyapunov exponents on the side of the orbit closest to the Earth. The local Lyapunov exponents in both of these plots

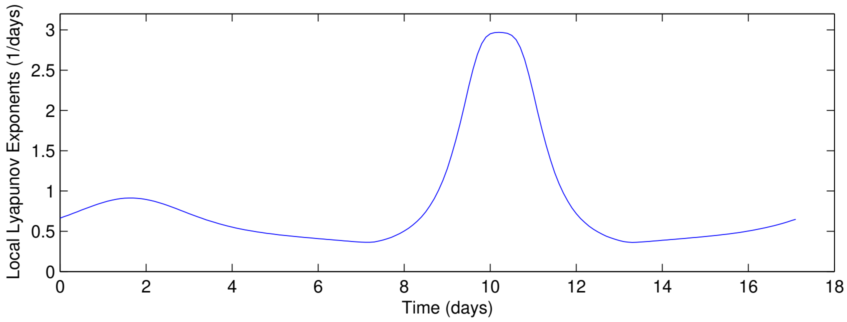

Figure 4 Local Lyapunov Exponents Versus Time for the Orbit in Figure 3

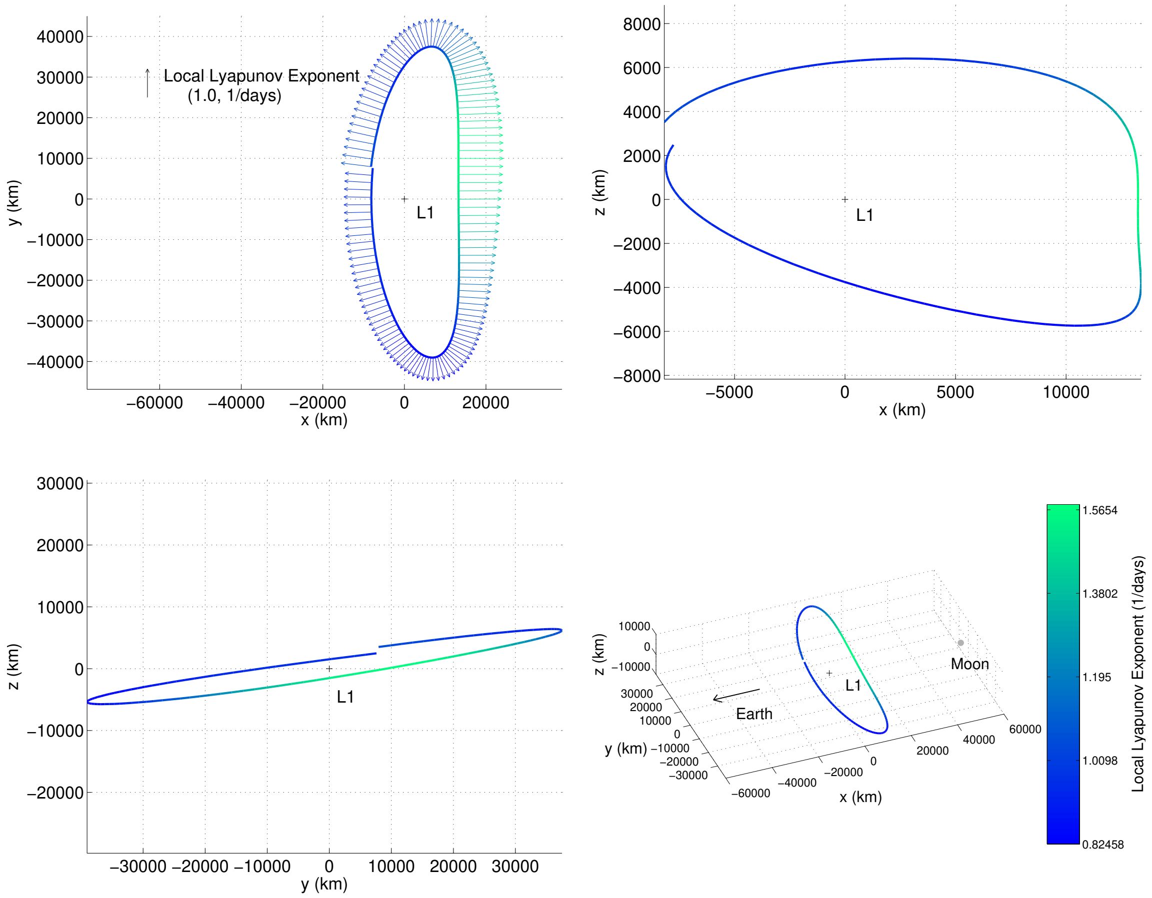

Figure 5 Local Lyapunov Exponents Calculated Over One-Day Intervals on a Lissajous Orbit in the Earth-Moon System using Ephemerides

generally increase on the portions of the trajectory that are closest to the Earth and Moon. In these cases, the most obvious increase is on the portion of the trajectory near the Moon. Similar trends were found in other quasi-periodic orbits around LL1. It has been observed that maneuvers on halo and Lissajous orbits appear to be most effective when they take place near the line connecting the primaries.[21] The increase in the local Lyapunov exponents near these areas does indeed indicate that perturbations or ΔVs would have a greater effect and may provide an explanation for why this occurs. Another area of exploration re-

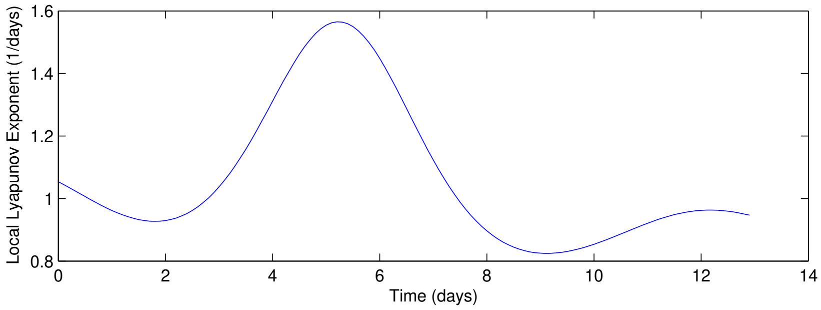

Figure 6 Time History of Local Lyapunov Exponents for the Lissajous Orbit in Figure 5

lates to how the local Lyapunov exponents vary if the time interval used in the calculation is increased. Figure 7 shows such a case for a time interval of 20 days. Generally as the time interval is increased, the variation between the peaks and valleys becomes smaller, and the local Lyapunov exponent begins to approach a single value. By comparing the scales on the plots in Figures 6 and 7, it can be seen that the curve using the 20-day interval is relatively flat. It is interesting to note that the larger peak in this plot occurs on the side of the orbit closest to the Earth. The smaller time intervals appear to be more appropriate for the focus of this study.

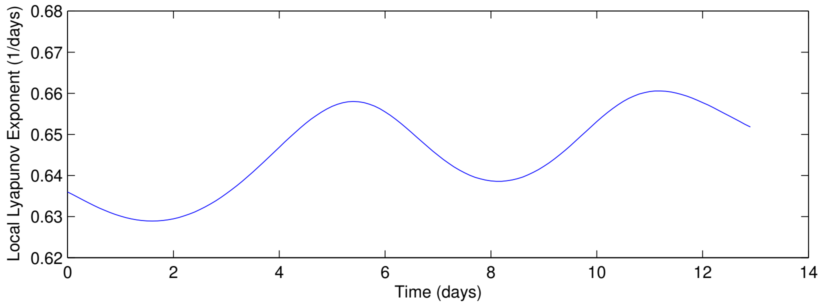

Figure 7 Time History of Local Lyapunov Exponents Calculated Over 20-Day Intervals for the Orbit in Figure 5

Comparison with Perturbations and Navigation Applications

The magnitude of the local Lyapunov exponents should indicate how perturbations will affect a trajectory, so a comparison of the local Lyapunov exponents and the effect of perturbations in phase space was performed. In each case, a perturbation in position and velocity was introduced at the same point that a local Lyapunov exponent was computed. The nominal and perturbed trajectories were then integrated forward for a time interval equal to that used in the calculation of the local Lyapunov exponent. The difference in position between the two integrated trajectories at the end of the time period was computed and compared with the local Lyapunov exponent. This concept is illustrated in Figure 8

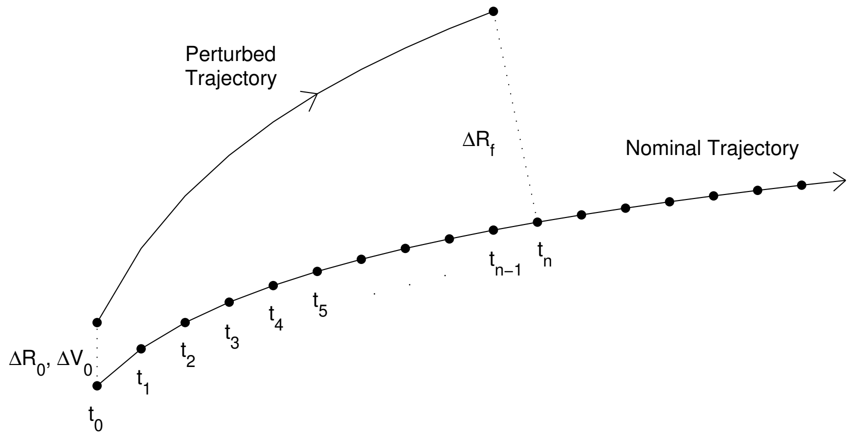

Figure 8 Illustration of Random Perturbation Calculation

where a single perturbation in position and velocity (ΔR_0 and ΔV_0) is shown at the first time (t_0) along with the final difference in position (ΔR_f). The time interval between the local Lyapunov exponent calculations ($t_n - t_{n-1}$) was typically 0.1 days, while the time interval used in the local Lyapunov exponent calculation ($t_n - t_0$) varied from 0.25 to three days. In the actual calculation, multiple random perturbations were introduced at each time.

For this study, a nearly planar Lyapunov orbit computed with the ephemerides of the Earth and Moon was used. The resulting orbit is shown in Figure 9 where the arrows once again represent the local Lyapunov exponents, and the results are given over time in Figure 10. For each point on the orbit where a local Lyapunov exponent was calculated,

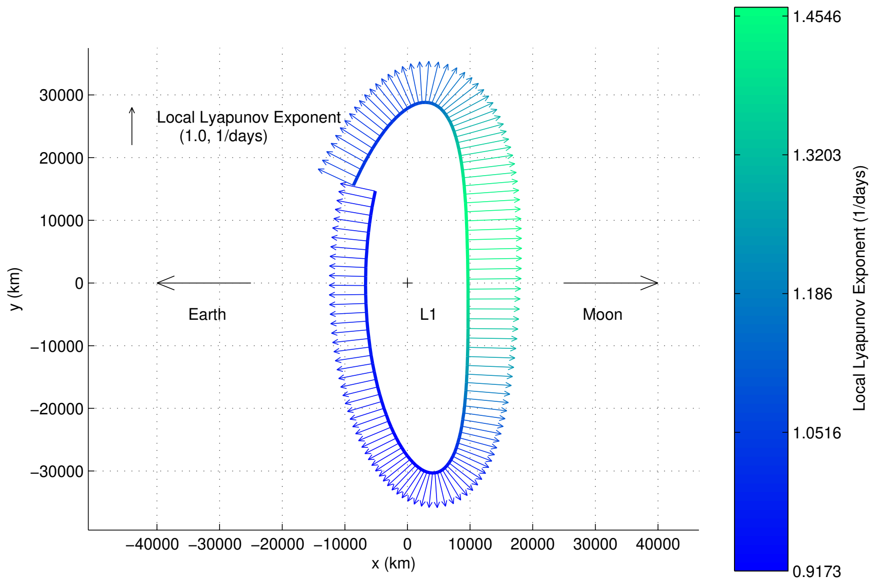

Figure 9 Local Lyapunov Exponents Plotted on a Nearly Planar Lyapunov Orbit Obtained with Ephemerides using a One-Day Interval

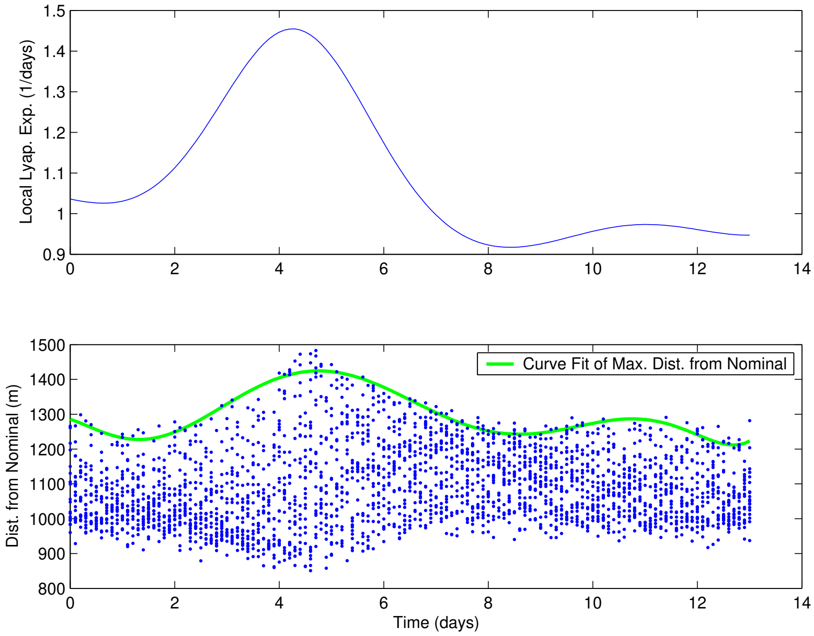

Figure 10 Local Lyapunov Exponents Plotted on the Lyapunov Orbit using a One-Day Interval (top), Final Distance From the Nominal as a Result of Random Perturbations with Magnitudes of 1 km and 1 mm/s (bottom)

20 different perturbations were introduced. These perturbations could be deviations from the nominal trajectory caused by ΔVs or other forces, and they could also be related to spacecraft state uncertainties. The final distances from the nominal trajectory were then computed and plotted in Figure 10 along with a curve fit of the final maximum distance from the nominal. The peaks and valleys in the maximum ΔV varied somewhat depending on the number of random points used and the curve fit. Generally, though, the peaks and valleys of the two curves tended to occur at approximately the same times. Overall, it was found that the trend in the local Lyapunov exponents corresponded very well with the final maximum distance between the nominal and the perturbed trajectories. This correspondence with the maximum distance rather than some other quantity is to be expected since the local Lyapunov exponent used here selects for the maximum growth of the perturbation. It may also be noted that the minimum distance is obtained near the peak of the local Lyapunov exponent. It appears that the direction of the random perturbation in phase space does have an effect then, but a large local Lyapunov exponent indicates that an unknown perturbation could have a greater impact at this point. If a trajectory must remain within some distance of the nominal, it would be desirable to ensure that uncertainties were smaller at the maximum local Lyapunov exponent so that any necessary maneuvers could be performed. The local stability characteristics are sometimes examined[17] by using the eigenvalues of the state transition matrix rather than utilizing the operator norm as given by Oseledec. A comparison between these two techniques was made, and it was found that for the orbits used in this study the trends for the two techniques were generally the same. So in order to further examine the effect of direction on a perturbation and how this

relates to local Lyapunov exponents, a case was run where a perturbation was made at each local Lyapunov exponent calculation in the direction of the eigenvector corresponding to the maximum eigenvalue of the state transition matrix. The final distance between the perturbed and nominal trajectory for this case corresponded very well to the trends found in the local Lyapunov exponents as can be seen by comparing the curves in Figure 11. Overall, it appears that the local Lyapunov exponents give a good indication of the maximum effect that a perturbation may have, but the direction of the perturbations plays a significant role. This result is not surprising since it is known that the dynamics around these unstable orbits are hyperbolic in nature.

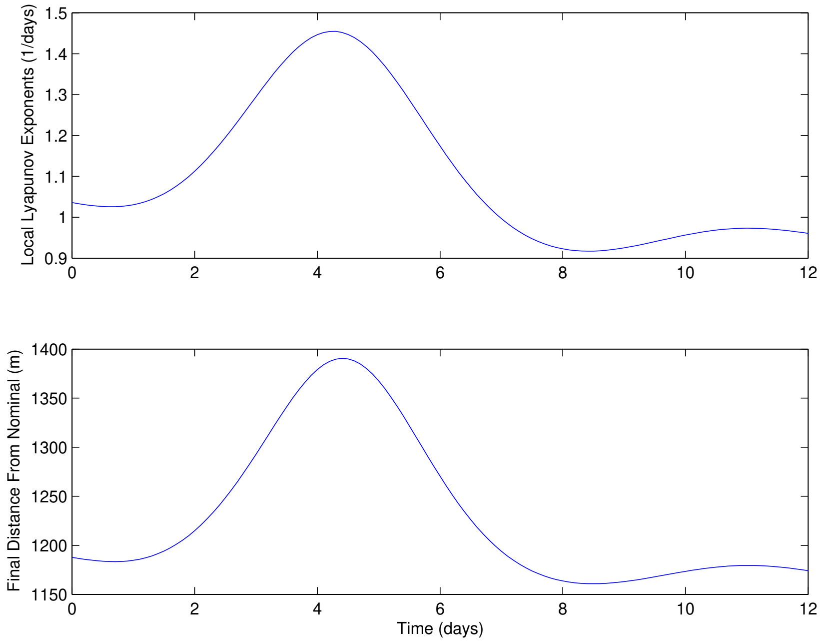

Figure 11 Local Lyapunov Exponents (top), Distance Traveled After One-Day for a Perturbation with an Initial Position Magnitude of 1 km in the Unstable Direction (bottom)

As previously mentioned, knowledge of the effect of perturbations given by local Lyapunov exponents have several straightforward applications to navigation uncertainties. Since equivalent perturbations can have varying effects at different points on a trajectory, it would be desirable to reduce uncertainties at the points on the trajectory where these effects are largest. This information could aid in scheduling observations in order to achieve the desired uncertainties. Devising a method for determining where observations should take place would be an area for further research.

Maneuver Design

The analysis of perturbations to a trajectory allowed the determination of locations where a perturbation or ΔV would cause a spacecraft to travel away from its nominal trajectory. The question then arises as to whether local Lyapunov exponents can be used as an indicator of the ΔV that would be required to return to the nominal trajectory from some perturbed trajectory. This would relate directly to maneuver design and stationkeeping for unstable orbits. As a method of comparing the local Lyapunov exponents and ΔVs, the total ΔV required to return to the nominal trajectory and match velocities over the time interval used in the local Lyapunov exponent calculation was computed. As in the previous comparison, 20 random perturbations were introduced each time a local Lyapunov exponent was calculated. The targeting portion of LTool's differential corrector[22] was used to determine the ΔV required to return to the nominal trajectory within the desired time interval. The total ΔV included both the initial ΔV required to target the nominal trajectory as well as the ΔV required to match velocities at the end of the time period.

The simple case of a planar Lyapunov orbit in the CR3BP was initially chosen for this comparison. A corresponding orbit integrated using the ephemerides of the Earth and Moon is plotted in Figure 9. Initially, small perturbations with magnitudes of 1 km and 0.1 mm/s were used since it is expected that smaller perturbations would result in the best correlation with the local Lyapunov exponents. The time history over approximately one period of the calculated local Lyapunov exponents and ΔVs are given in Figure 12 for the case where

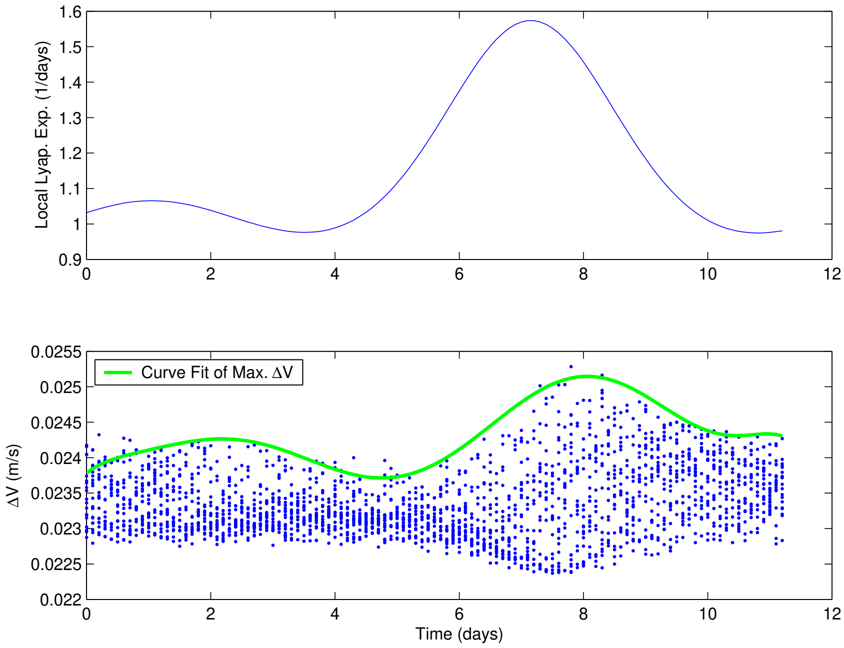

Figure 12 Local Lyapunov Exponents (top) and ΔVs (bottom) Calculated Over One-Day Intervals on a Lyapunov Orbit in the CR3BP with Perturbations of 1 km and 0.1 mm/s

the local Lyapunov exponents and the ΔVs were computed using one-day intervals. Both computations were performed at 0.1 day intervals for all the remaining cases. It can be seen from Figure 12 that the local Lyapunov exponents varied from approximately 0.97 to 1.57 days^{-1} with two peaks in their values. The larger peak corresponded as usual to the side of the orbit closest to the Moon. The ΔVs for each of the random perturbations are also plotted with the maximum ΔV having a value of 2.53 cm/s. These values are comparable to the magnitude of the stationkeeping ΔVs used in other studies.[8] The local Lyapunov exponents in this case appeared to have the best correlation with the maximum computed ΔVs at each point. The outliers were removed from these values, and a curve fit of the main ΔVs was computed as given in the figure. Although the shape of the curves appears to be similar, the peaks and valleys occur at different times. By comparing the times of the largest peak, it can be seen that the maximum ΔV peak occurs approximately 0.9 days after the peak in the local Lyapunov exponents. The second highest maximum ΔV peak occurs nearly one day after the local Lyapunov exponents peak, and the deepest valley occurs approximately 1.1 days after the local Lyapunov exponents. From this comparison, it appears that the maximum ΔV curve trails the local Lyapunov exponent curve by approximately one day, or the length of time used in the local Lyapunov exponent calculation. It may be that the maximum ΔV and the local Lyapunov exponent should be compared at the end of the local Lyapunov exponent calculation when the spacecraft is nearest the nominal trajectory, and the final ΔV is performed.

In order to test this hypothesis and examine the effect on the comparison of varying the time interval used in the calculation, several cases were used with different time intervals. For the first of these cases, shown in Figure 13, the time interval was reduced to 0.25

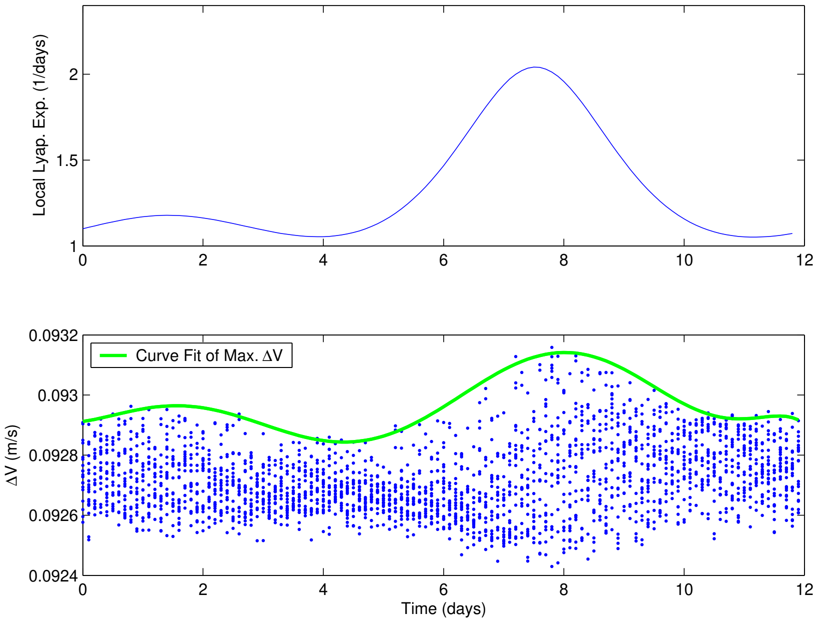

Figure 13 Local Lyapunov Exponents (top) and ΔVs (bottom) Calculated Over 0.25-Day Intervals on a Lyapunov Orbit in the CR3BP with Perturbations of 1 km and 0.1 mm/s

days. Here, it is more difficult to locate the peaks and valleys in the data to sufficient accuracy, but the offsets appear to be consistent with the new time interval of 0.25 days. It may also be noticed that the local Lyapunov exponents and the ΔVs are both larger for this case. If the local Lyapunov exponent equation is examined, it can be seen that the local Lyapunov exponent is inversely proportional to the time interval, so the smaller time interval would tend to increase the local Lyapunov exponent. The larger ΔVs can be expected because the requirements are now more stringent. The spacecraft has less time to return to the nominal trajectory even though the magnitude of the perturbations has not changed. Next, a case using a time interval of two days was used, and the results are plotted in Figure 14. It may be noted that the local Lyapunov exponents are not computed to the end

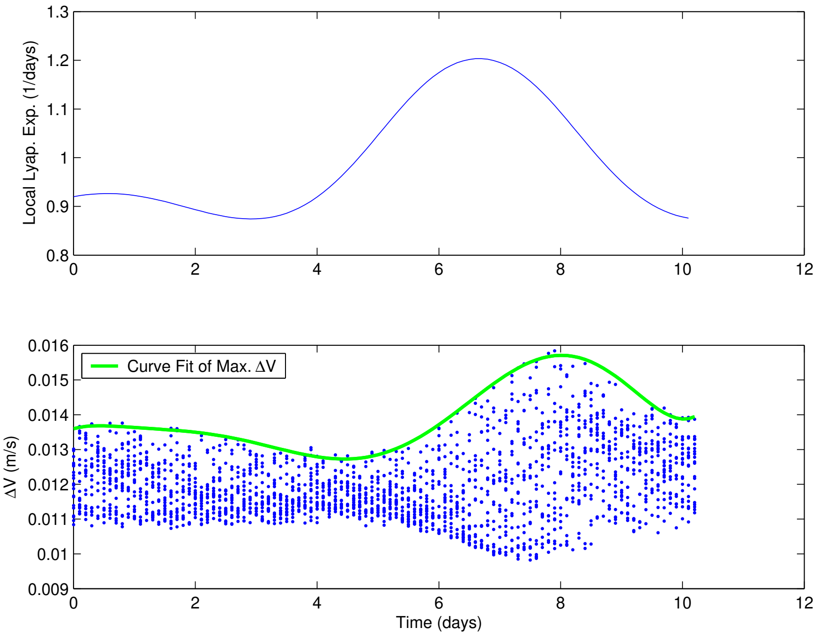

Figure 14 Local Lyapunov Exponents (top) and ΔVs (bottom) Calculated Over Two-Day Intervals on a Lyapunov Orbit in the CR3BP with Perturbations of 1 km and 0.1 mm/s

of the period because two days worth of data were needed to compute the local Lyapunov exponents. As expected, the magnitude of the local Lyapunov exponents and the maximum ΔVs has decreased even further in this plot. Comparing the peaks and valleys of the plot reveals that the maximum ΔVs are approximately 1.6-1.8 days behind the local Lyapunov exponents depending on the curve fit that is used. If the time interval is increased even further to three days, as shown in Figure 15, the peaks in the maximum ΔV plot lag those on the local Lyapunov exponent plot by approximately 0.75 days. Therefore, it appears that some relationship may exist between the offset in the maximum ΔV and local Lyapunov exponent plot for time intervals on the order of one day, but it is not as clearly defined for time intervals of two days. The relationship begins to fall apart for larger time intervals. However, in each case the offset between the two curves appears to be nearly constant. Once this offset is known, the local Lyapunov exponents could then be easily used as an indicator of required maximum ΔV.

Several other questions remain in relation to the applicability of this technique. An additional test was to determine if the previously examined relationships exist for larger perturbations. The case for one-day intervals using perturbations with magnitudes of 10 km and 1 mm/s is shown in Figure 16. This results in a maximum ΔV of 25.2 cm/s, and the

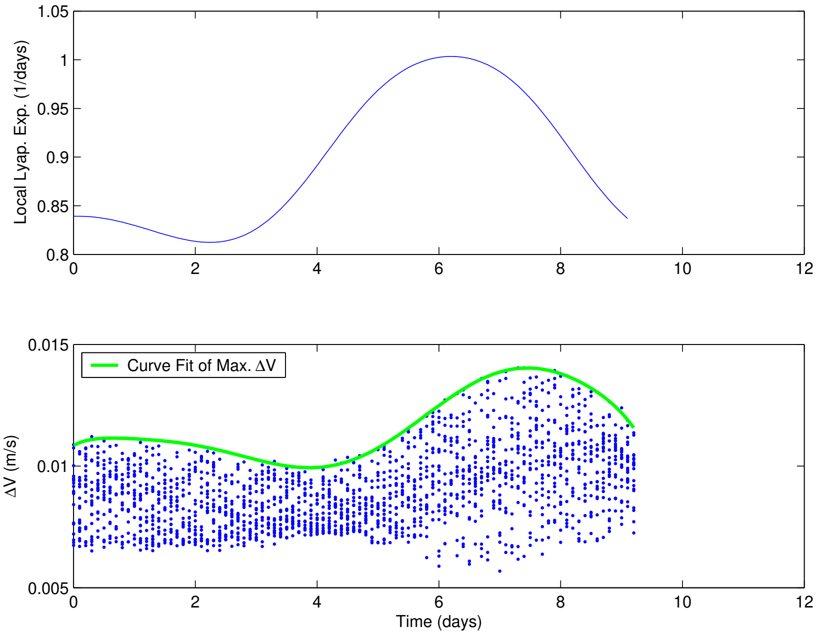

Figure 15 Local Lyapunov Exponents (top) and ΔVs (bottom) Calculated Over Three-Day Intervals on a Lyapunov Orbit in the CR3BP with Perturbations of 1 km and 0.1 mm/s

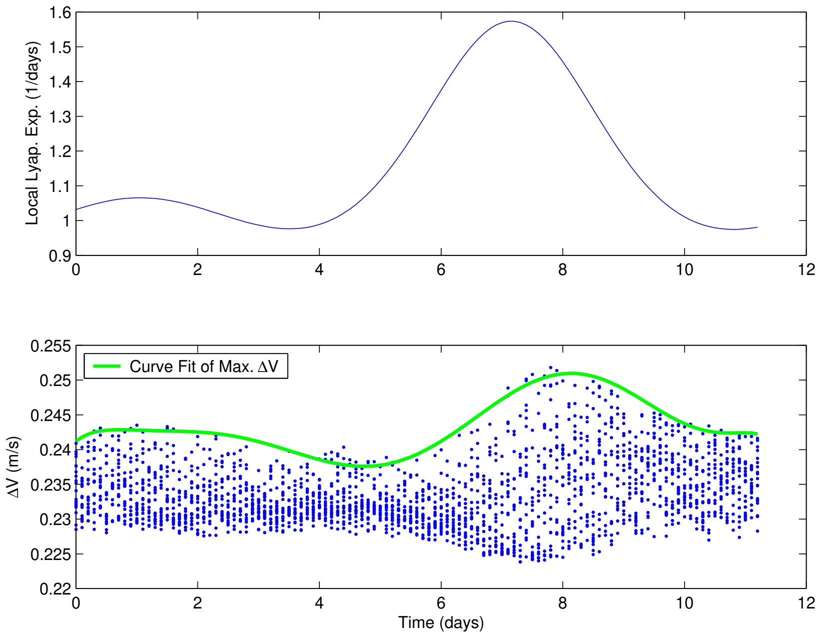

Figure 16 Local Lyapunov Exponents (top) and ΔVs (bottom) Calculated Over One-Day Intervals on a Lyapunov Orbit in the CR3BP with Perturbations of 10 km and 1.0 mm/s

curve had nearly the same shape as seen in the plot using smaller perturbations. Once again, the offset between the two curves was approximately one day. An additional test was to determine how the ΔVs behaved for a nonplanar orbit integrated with the full ephemerides of

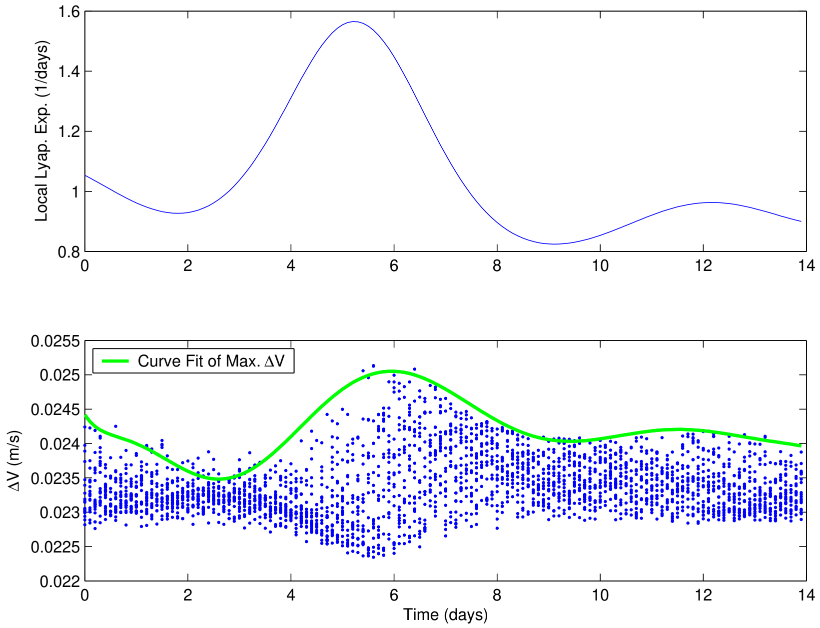

Figure 17 Local Lyapunov Exponents (top) and ΔVs (bottom) Calculated Over One-Day Intervals on a Lissajous Orbit Using Ephemerides with Perturbations of 1 km and 0.1 mm/s

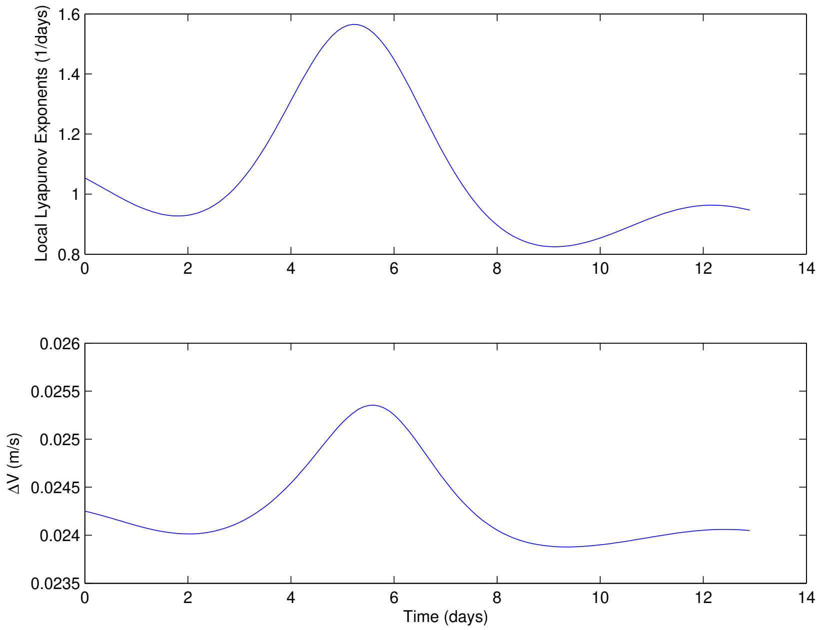

Figure 18 Local Lyapunov Exponents (top) and ΔVs (bottom) Calculated Over 0.25-Day Intervals on a Lissajous Orbit Using Ephemerides in the Unstable Direction with Perturbations of 1 km

the Earth and Moon. The results for the Lissajous orbit in Figure 5 are shown in Figure 17. Here, the relationship between the two curves generally remains the same. The offset in the peaks of the two curves can be estimated as approximately one day. The second valley at nearly 10 days in the maximum ΔV curve is not as noticeable as in the local Lyapunov exponent curve, but it still seems to exist. Finally, a comparison with the ΔVs required for a perturbation in the unstable direction of the state transition matrix was performed. The results for the case with an interval of 0.25 days are shown in Figure 18. It appears that the same trends found in the maximum ΔV using the random perturbations also exist in this curve.

CONCLUDING REMARKS

The behavior of local Lyapunov exponents have been partially numerically characterized on periodic and quasi-periodic orbits in the CR3BP and using models which include the ephemerides of the Earth and Moon. Numerical comparisons with random perturbations and possible stationkeeping maneuvers have been performed. It was found that local Lyapunov exponents generally increase on the portion of the selected orbits that came closest to the Earth and Moon with the largest peak occurring on the side of the orbit closest to the Moon. This corresponds to locations in the orbit most perturbed by the gravitating bodies. This information agrees well with observations that maneuvers are generally more effective along the line connecting the two primaries. A comparison of the local Lyapunov exponents with the effect of random perturbations on the separation between the perturbed and the nominal trajectory revealed that the local Lyapunov exponents best matched the trend in the maximum separation. With this information, the local Lyapunov exponents can be used to indicate where it would be most important to reduce the magnitude of navigation uncertainties. The local Lyapunov exponents also matched perturbations made in the unstable direction of the state transition matrix, which along with the previous comparisons, shows that the direction of the perturbation plays a significant role in its behavior.

The comparison of local Lyapunov exponents and ΔVs required to return to a trajectory from a random perturbation showed that the trends in the local Lyapunov exponents generally matched those of the maximum required ΔV. However, an offset in time exists that corresponds to the time interval used in the local Lyapunov exponent calculation for time intervals less than two days in length for the Earth-Moon system, and some constant offset for larger time intervals. With knowledge of this offset, the local Lyapunov exponents can be used as a method for selecting the desired locations to perform maneuvers. This correlation was also found to exist for large ΔVs of approximately 20 cm/s as well as for the original ΔVs of approximately 2 cm/s. The comparison also remained valid for Lissajous orbits in the three-body problem and Lyapunov orbits in the CR3BP.

Future work will include an examination of techniques for incorporating the direction of the perturbation into the process. The relationship with navigation uncertainties will also be further examined. These methods can be extended to additional trajectories in the three-body problem as well as continuous thrust trajectories like those used for the Jupiter Icy Moons Orbiter (JIMO). Eventually it would be desirable to automate the navigation and maneuver design process along unstable orbits using these techniques.

ACKNOWLEDGMENTS

The authors would like to thank Randy Paffenroth for providing the AUTO2000 scripts used to generate the Lyapunov orbit initial condition for this study. They would also like to thank the AAS Breakwell Travel Award Committee for the funds used to travel to this conference and Bob Easton for his helpful discussions.

This work was conducted for the Jet Propulsion Laboratory, California Institute of Technology, under contract with the National Aeronautics and Space Administration.

REFERENCES

[1] Howell, K.C., B.T. Barden, R.S. Wilson, and M.W. Lo, "Trajectory Design Using a Dynamical Systems Approach with Application to GENESIS," AAS Paper 97-709, AAS/AIAA Astrodynamics Specialist Conference, August 4-7, 1997.

[2] Lo, M.W., B.G. Williams W.E. Bollman, D. Han, Y. Hahn, J.L. Bell, E.A. Hirst, R.A. Corwin, P.E. Hong, K.C. Howell, B. Barden and R. Wilson, "Genesis Mission Design," AIAA Paper No. 98-4468, AIAA Astrodynamics Conference, Boston, Massachusetts, August, 1998.

[3] Farquhar, R.W., D.P. Muhonen, C.R. Newman, and H.S. Heuberger, "Trajectories and Orbital Maneuvers for the First Libration-Point Satellite," *Journal of Guidance and Control*, Vol. 3, No. 6, Nov.-Dec., 1980, pp. 549-554.

[4] Heuberger, H.S., "Halo Orbit Station Keeping for International Sun-Earth Explorer-C (ISEE-C)," AAS/AIAA Astrodynamics Specialist Conference, Grand Teton National Park, Wyoming, September 7-9, 1977.

[5] Howell, K.C. and H.J. Pernicka, "Stationkeeping Method for Libration Point Trajectories," *Journal of Guidance, Control, and Dynamics*, Vol. 16, No. 1, January-February, 1993, pp. 151-159.

[6] Scheeres, D.J. and C. Renault, "Optimal Placement of Statistical Maneuvers in an Unstable Orbital Environment," AAS/AIAA Astrodynamics Specialist Conference, Monterrey, California, August 2002.

[7] Gómez G., J. Llibre, R. Martnez, and C. Simó, *Dynamics and Mission Design Near Libration Points*, Vols. 1-4, World Scientific Monograph Series in Mathematics, Singapore, 2001.

[8] Gómez, G., K. Howell, J. Masdemont and C. Simó, "Station-Keeping Strategies for Translunar Libration Point Orbits," AAS Paper 98-168, AAS/AIAA Space Flight Mechanics Conference, Monterey, California, February 9-11, 1998.

[9] Bell, J.L., M.W. Lo, and R.S. Wilson, "Genesis Trajectory Design," AAS/AIAA Astrodynamics Specialist Conference, Girdwood, Alaska, August 16-19, 1999.

[10] Lyapunov A.M., *The General Problem of the Stability of Motion*, Comm. Soc. Math. Kharkow (in Russian, reprinted in English, Taylor & Francis, London, 1992), 1892.

[11] Oseledec, V.I., "A Multiplicative Ergodic Theorem. Lyapunov Characteristic Numbers for Dynamical Systems," Trudy Moskov. Mat. Obsc. 19, Transactions of the Moscow Mathematical Society, Vol. 19, 1968, pp. 197-231.

[12] Abarbanel, H.D.I., R. Brown, and M.B. Kennel, "Variation of Lyapunov Exponents on a Strange Attractor," *Journal of Nonlinear Science*, Vol. 1, 1991, pp. 175-199.

[13] Froeschlé, C., E. Lohinger, and E. Lega, "On the Relationship Between Local Lyapunov Characteristic Numbers, Largest Eigenvalues and Maximum Stretching Parameters," *The Dynamics of Small Bodies in the Solar System*, B.A. Steves and A.E. Roy, Kluwer Academic Publishers, The Netherlands, 1999.

[14] Lichtenberg, A.J. and M.A. Lieberman, *Regular and Stochastic Motion*, Springer-Verlag, New York, 1983.

[15] Parker, T.S. and L.O. Chua, *Practical Numerical Algorithms for Chaotic Systems*, Springer-Verlag, New York, 1989.

[16] Pollicott, M., *Lectures on Ergodic Theory and Pesin Theory on Compact Manifolds*, London Math. Society Lecture Notes Series 180, Cambridge University Press, 1993.

[17] Scheeres, D.J., "Characterizing the Orbit Uncertainty Dynamics along an Unstable Orbit," AAS Paper 01-302, AAS/AIAA Astrodynamics Specialist Conference, Quebec City, July 30 - August 2, 2001.

[18] Giorgini, J.D., Yeomans, D.K., Chamberlin, A.B., Chodas, P.W., Jacobson, R.A., Keesey, M.S., Lieske, J.H., Ostro, S.J., Standish, E.M., Wimberly, R.N., "JPL's On-Line Solar System Data Service," *Bulletin of the American Astronomical Society* 28(3), 1158, 1996.

[19] Richardson, D.L. and N.D. Cary, "A Uniformly Valid Solution for Motion About the Interior Libration Point of the Perturbed Elliptic-Restricted Problem," Paper AAS 75-021, AAS/AIAA Astrodynamics Specialist Conference, Nassau, Bahamas, July 28-30, 1975.

[20] Paffenroth, R.C., E.J. Doedel, D.J. Dichmann, "Continuation of Periodic Orbits Around Lagrange Points and AUTO2000," Paper AAS 01-303, AAS/AIAA Astrodynamics Specialist Conference, Quebec City, July 30 - August 2, 2001.

[21] Dunham, D., Personal Communications, 2003.

[22] Roby, S.W., "Derivation of Differential Correctors Used in GENESIS Mission Design," JPL IOM 312.I-03-002, 2003.